Proc. Natl. Acad. Sci. USA
Vol. 92, pp. 9323–9327, September 1995
Cell Biology

12(*S*)-Hydroxyeicosatetraenoic acid and 13(*S*)-hydroxyoctadecadienoic acid regulation of protein kinase C-α in melanoma cells: Role of receptor-mediated hydrolysis of inositol phospholipids

(monohydroxy fatty acids/signaling/tumor cells)

BIN LIU*†, WASIUDDIN A. KHAN‡§, YUSUF A. HANNUN‡§, JOZSEF TIMAR*, JOHN D. TAYLOR*¶, STEVEN LUNDY*, IGOR BUTOVICH*, AND KENNETH V. HONN*,‖,**,††

Departments of *Radiation Oncology, ¶Biological Sciences, ‖Chemistry, and **Pathology, Wayne State University, Detroit, MI 48202; and Departments of ‡Medicine and §Cell Biology, Duke University Medical Center, Durham, NC 27710

Communicated by Petro Cuatrecasas, Parke–Davis, Ann Arbor, MI, March 9, 1995

ABSTRACT **Protein kinase C (PKC) isoenzymes are essential components of cell signaling. In this study, we investigated the regulation of PKC-α in murine B16 amelanotic melanoma (B16a) cells by the monohydroxy fatty acids 12(*S*)-hydroxyeicosatetraenoic acid [12(*S*)-HETE] and 13(*S*)-hydroxyoctadecadienoic acid [13(*S*)-HODE]. 12(*S*)-HETE induced a translocation of PKC-α to the plasma membrane and focal adhesion plaques, leading to enhanced adhesion of B16a cells to the matrix protein fibronectin. However, 13(*S*)-HODE inhibited these 12(*S*)-HETE effects on PKC-α. A receptor-mediated mechanism of action for 12(*S*)-HETE and 13(*S*)-HODE is supported by the following findings. First, 12(*S*)-HETE triggered a rapid increase in cellular levels of diacylglycerol and inositol trisphosphate in B16a cells. 13(*S*)-HODE blocked the 12(*S*)-HETE-induced bursts of both second messengers. Second, the 12(*S*)-HETE-increased adhesion of B16a cells to fibronectin was sensitive to inhibition by a phospholipase C inhibitor and pertussis toxin. Finally, a high-affinity binding site (K_d = 1 nM) for 12(*S*)-HETE was detected in B16a cells, and binding of 12(*S*)-HETE to B16a cells was effectively inhibited by 13(*S*)-HODE (IC_{50} = 4 nM). In summary, our data provide evidence that regulation of PKC-α by 12(*S*)-HETE and 13(*S*)-HODE may be through a guanine nucleotide-binding protein-linked receptor-mediated hydrolysis of inositol phospholipids.**

Protein kinase C (PKC) consists of a family of protein-serine/threonine kinases that play important roles in mediating cell growth, differentiation, and tumor promotion (1). Binding of extracellular stimulators (e.g., hormones, growth factors, cytokines, and neurotransmitters) to their cell surface receptors triggers the phospholipase C (PLC)-mediated hydrolysis of phosphatidylinositol bisphosphate, generating the second messengers diacylglycerol (DAG) and D-*myo*-inositol 1,4,5-trisphosphate (IP_3). While DAG directly activates PKC, IP_3 releases Ca^{2+} from intracellular stores (1). Tumor-promoting phorbol esters, such as phorbol 12-myristate 13-acetate (PMA), mimic DAG and directly activate PKC.

Metastasis is a multistep process involving tumor cell detachment from the primary tumor, invasion through basement membrane, and intravasation (2). Once blood borne, the tumor cell must adhere to endothelium, induce endothelial cell retraction, and again invade through basement membrane to form a successful secondary tumor. Previously, we have observed that the ability of tumor cells to accomplish many of these steps in the metastatic cascade is enhanced by 12(*S*)-hydroxyeicosatetraenoic acid [12(*S*)-HETE], a lipoxygenase metabolite of arachidonic acid; the 12(*S*)-HETE effects are antagonized by 13(*S*)-hydroxyoctadecadienoic acid [13(*S*)-HODE], a lipoxygenase metabolite of linoleic acid (3, 4). Inhibitor studies revealed that PKC was involved in basal and 12(*S*)-HETE-regulated tumor cell and endothelial cell integrin expression (5), adhesion (6, 7), spreading (5), and experimental metastasis (7). However, the involvement of specific PKC isoform(s) and particularly the related mechanism(s) of action for 12(*S*)-HETE and 13(*S*)-HODE have not been explored.

Previously, exploration of mechanisms of action for mono-HETEs placed emphasis on investigating their fate after uptake by cells and their intracellular targets. For example, extracellular mono-HETEs are esterified into phospholipids, possibly affecting certain membrane functions (8). *In vitro* kinase assays revealed that 15-HETE can increase PKC activity (9), and 12-HETE can activate PKC-γ (10). Finally, incorporated 12(*S*)-HETE has been shown to bind to an intracellular protein (11). Although receptors have been identified for some eicosanoids (12–18), studies on possible cell membrane receptor-mediated signaling processes for 12(*S*)-HETE and/or 13(*S*)-HODE are lacking. In this study, we propose that 12(*S*)-HETE and 13(*S*)-HODE interact with a cell surface receptor(s) whose activation leads to generation of second messengers and further downstream activation of PKC.

MATERIALS AND METHODS

Materials. Polyclonal antibodies against PKC-α, -βI, -βII, -γ, -δ, -ε, or -ξ were prepared as described (19). PMA, pertussis toxin, and cholera toxin were obtained from Calbiochem. Genistein was purchased from Sigma. 12(*S*)-[^{3}H]HETE (215.3 Ci/mmol; 1 Ci = 37 GBq) was from NEN. Murine B16 amelanotic melanoma (B16a) cells were maintained as described (5).

Subcellular Fractionation, PKC Activity Assay, and Western Blotting. Cytosol and membrane PKC were prepared and partially purified with DEAE-Sephacel (Sigma) as described (6). Cytoskeleton was prepared from the detergent-insoluble membrane pellet by washing twice in buffer containing 1% Nonidet P-40, 0.15 M NaCl, and 0.1 M KCl. Protein concentration was determined by the Bio-Rad detergent-compatible

The publication costs of this article were defrayed in part by page charge payment. This article must therefore be hereby marked "*advertisement*" in accordance with 18 U.S.C. §1734 solely to indicate this fact.

Abbreviations: B16a, B16 amelanotic melanoma; DAG, 1,2-diacyl-*sn*-glycerol; HETE, hydroxyeicosatetraenoic acid; HODE, hydroxyoctadecadienoic acid; IP_3, D-*myo*-inositol 1,4,5-trisphosphate; PKC, protein kinase C; PLC, phospholipase C; PMA, phorbol 12-myristate 13-acetate; G protein, guanine nucleotide-binding protein; PS, phosphatidylserine.

†Present address: Duke University Medical Center, Box 3355, Durham, NC 27710.
††To whom reprint requests should be addressed at: 431 Chemistry Building, Wayne State University, Detroit, MI 48202.

protein assay reagents using bovine serum albumin (Sigma) as the standard. PKC activity was determined as described (6) by measuring the incorporation of $^{32}P_i$ from [γ-^{32}P]ATP to histone H1 in the presence or absence of 0.75 mM Ca^{2+}, 24 μg of phosphatidylserine (PS), and 1.6 μg of 1,2-dioleoyl-*sn*-glycerol. For Western blotting, samples were separated on an SDS/10% polyacrylamide gel under reducing conditions and electrophoretically transferred to nitrocellulose. Blotting for PKC was performed as described (19) except that the bound antibody was detected with the ECL Western blotting reagents (Amersham).

***In Vitro* Activation of PKC.** Baculovirus-expressed PKC-α was purified as described (20). Assay of the enzyme was carried out in PS/DAG vesicles containing 20 mM Tris·HCl (pH 7.5), 10 mM $MgCl_2$, 10 μM ATP, histone H1 (200 μg/ml), 50 μM PS, 3.4 μM 1,2-dioleoyl-*sn*-glycerol, and 400 μM Ca^{2+} in a final volume of 250 μl as described (21). Indicated concentrations of 12(*S*)-HETE were added in 1 μl of ethanol.

Immunofluorescent Studies. Detection of plasma membrane-associated PKC was performed as described (6). For labeling PKC (6) or vinculin (5) in focal adhesion plaques, cells grown on fibronectin-coated coverslips were fixed with paraformaldehyde and permeabilized with 0.5% Triton X-100, labeled with anti-PKC or anti-vinculin antibody (Boehringer Mannheim), and then labeled with biotinylated goat anti-mouse IgG and streptavidin-Texas Red (30 min). Omission of primary antibody or incubation with an inappropriate primary antibody gave negligible background staining. For visualization, the coverslips were mounted with Citifluor (Ted Pella, Redding, CA), and immunofluorescent images were recorded with a Nikon Optiphot-2 microscope equipped with a G-2A or B-2A filter.

Adhesion of B16a Cells to Fibronectin. Cells (10^4 per well) were incubated for 45 min with fibronectin (5 μg per well)-coated 96-well cell plates (Corning). After removing nonadherent cells, the adherent cells were fixed with 4% (wt/vol) paraformaldehyde. Cells in three constant unit areas (240 μm^2) were visually counted with a Nikon inverted-phase contrast microscope.

DAG and IP_3 Assay. The amount of DAG was determined with an assay kit (Amersham) that is based on the quantitative conversion of DAG to [^{32}P]phosphatidic acid. Cell lipids were extracted according to the method of Bligh and Dyer (22), and [^{32}P]phosphatidic acid was purified with a silica gel TLC plate with chloroform/methanol/acetic acid (65:15:5, vol/vol). Radioactivity was determined by liquid scintillation spectrometry. The amount of IP_3 was determined with a competitive binding assay kit (Amersham) after extraction with perchloric acid.

Binding Assay. For binding assays, confluent monolayers of B16a cells in 24-well culture plates were washed four times with serum-free MEM and cooled to 4°C. 12(*S*)-[^{3}H]HETE (400 μl of medium per well) was added, and the plate was kept under constant and gentle shaking at 4°C for the desired time intervals. Incubation was terminated by washing the cells four times with ice-cold PBS. The cells were solubilized with 0.1 M NaOH, and radioactivity was determined by liquid scintillation spectrometry. The dissociation constants and the number of binding sites per cell were determined by nonlinear regression analysis using the TABLE CURVE software (Jandel, San Rafael, CA). The following binding scheme represents the best fit of the data from three separate experiments:

$$L + Q_a \xrightarrow{K_{d1}} LQ_a \quad [1]$$

$$2L + Q_b \xrightarrow{K_{d2}} L_2Q_b, \quad [2]$$

where L is the ligand and K_{d1} and K_{d2} are dissociation constants for two separate receptors Q_a and Q_b of high and low affinity, respectively. The data fit the following equation: total bound ligand = $[(Q_a \times L)/(K_{d1} + L)] + [(Q_b \times L^2)/(K_{d2} + L^2)]$ with an $r^2 = 0.999$ and $F_{stat} = 1482$.

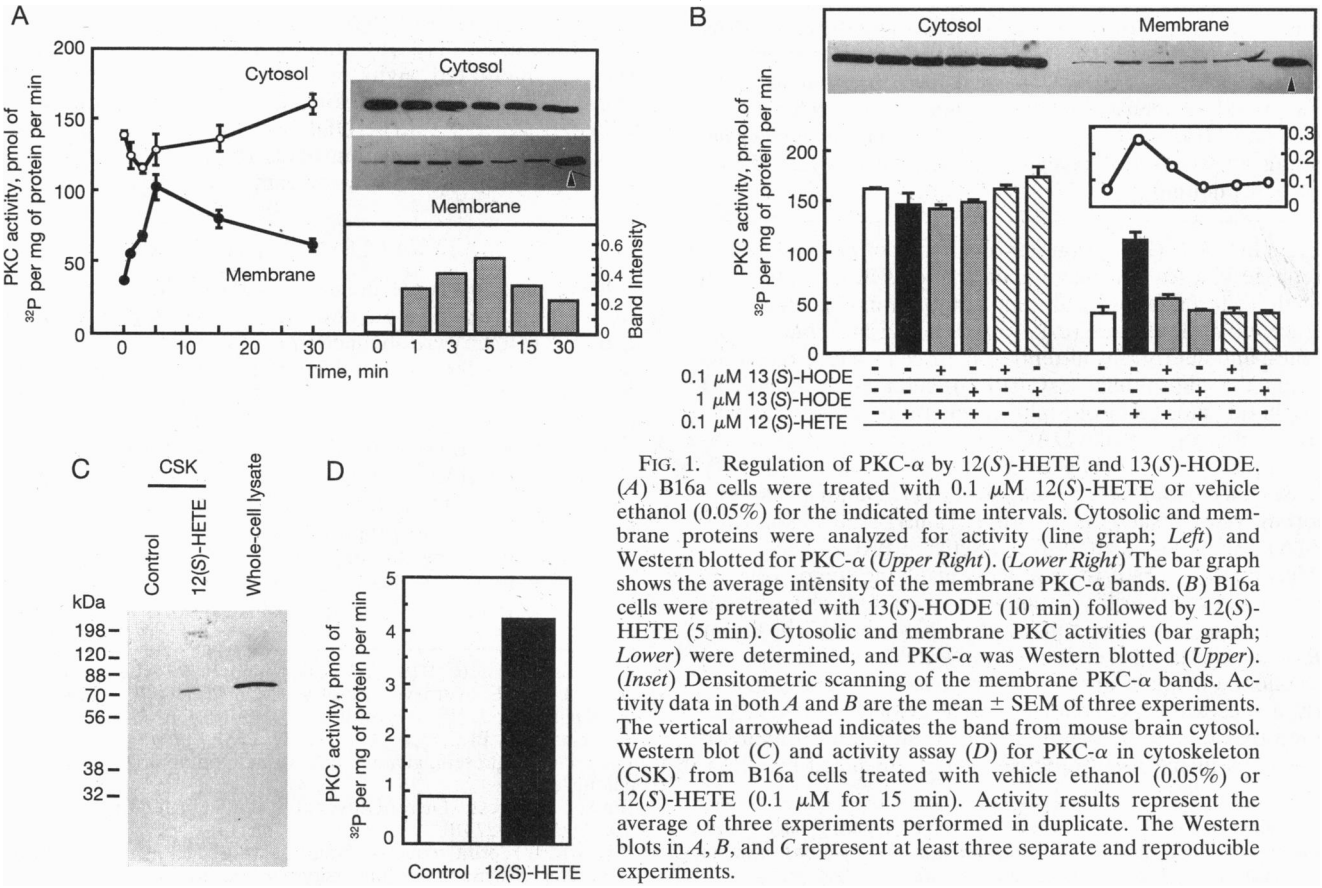

FIG. 1. Regulation of PKC-α by 12(*S*)-HETE and 13(*S*)-HODE. (*A*) B16a cells were treated with 0.1 μM 12(*S*)-HETE or vehicle ethanol (0.05%) for the indicated time intervals. Cytosolic and membrane proteins were analyzed for activity (line graph; *Left*) and Western blotted for PKC-α (*Upper Right*). (*Lower Right*) The bar graph shows the average intensity of the membrane PKC-α bands. (*B*) B16a cells were pretreated with 13(*S*)-HODE (10 min) followed by 12(*S*)-HETE (5 min). Cytosolic and membrane PKC activities (bar graph; *Lower*) were determined, and PKC-α was Western blotted (*Upper*). (*Inset*) Densitometric scanning of the membrane PKC-α bands. Activity data in both *A* and *B* are the mean ± SEM of three experiments. The vertical arrowhead indicates the band from mouse brain cytosol. Western blot (*C*) and activity assay (*D*) for PKC-α in cytoskeleton (CSK) from B16a cells treated with vehicle ethanol (0.05%) or 12(*S*)-HETE (0.1 μM for 15 min). Activity results represent the average of three experiments performed in duplicate. The Western blots in *A*, *B*, and *C* represent at least three separate and reproducible experiments.

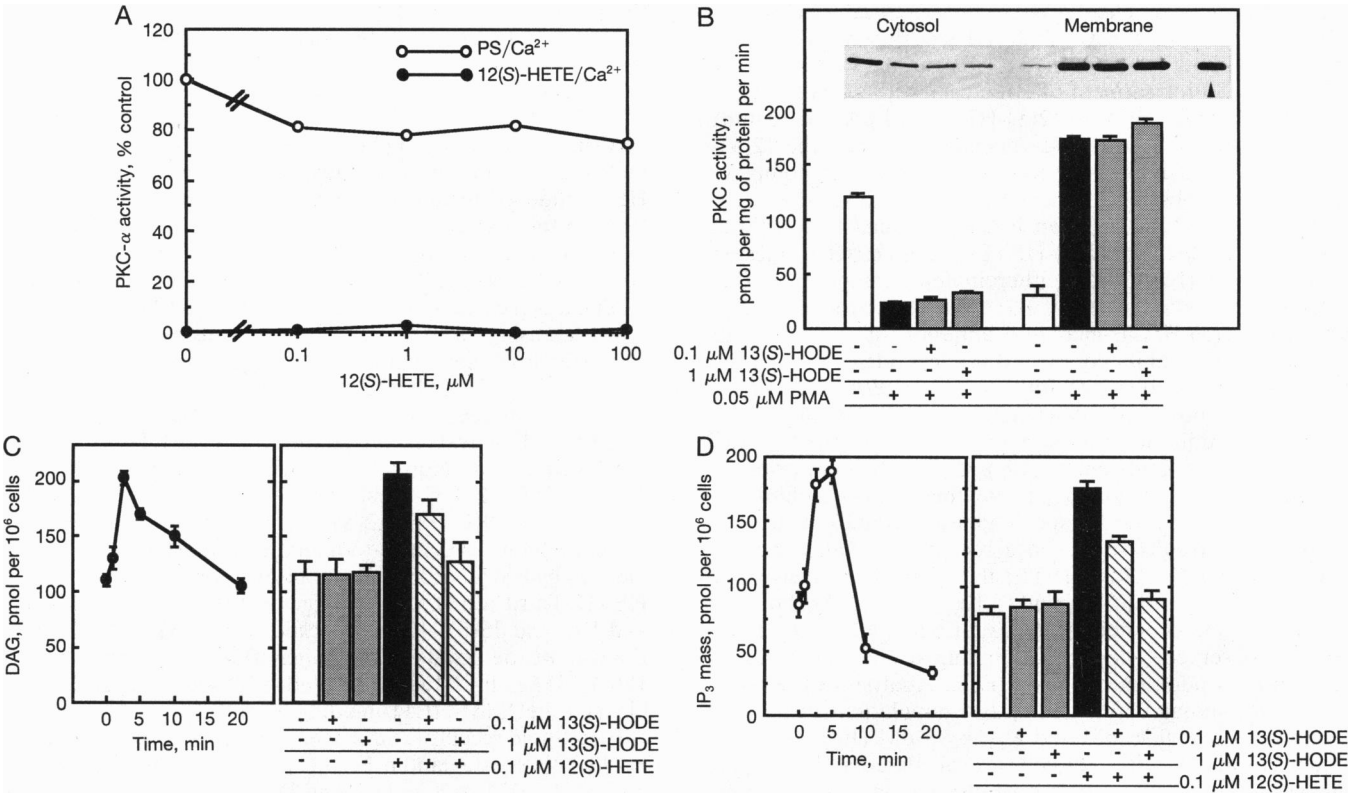

FIG. 2. Analysis of mechanism of action for 12(*S*)-HETE and 13(*S*)-HODE regulation of PKC-α. (*A*) Direct activation of PKC-α by 12(*S*)-HETE. Baculovirus-expressed PKC-α was assayed in a vesicle assay containing 50 μM PS and 3.4 μM DAG in the presence of the indicated concentrations of 12(*S*)-HETE. (*B*) Effect of 13(*S*)-HODE on PMA-induced membrane translocation of PKC-α. B16a cells were pretreated with 13(*S*)-HODE (10 min) followed by PMA treatment (50 nM for 10 min). (*Lower*) Cytosolic and membrane PKC activities were determined. (*Upper*) Western blot for cytosolic and membrane PKC-α. The vertical arrowhead indicates the band from mouse brain cytosol. (*C* and *D*) Effect of 12(*S*)-HETE and 13(*S*)-HODE on DAG and IP_3 formation in B16a cells. To determine the 12(*S*)-HETE effect, cells were treated with 0.1 μM 12(*S*)-HETE for the indicated time intervals. To determine the 13(*S*)-HODE effect, cells were treated (10 min) with 13(*S*)-HODE followed with or without 12(*S*)-HETE (0.1 μM for 2.5 min). Results are expressed as the mean ± SEM of three experiments performed in duplicate.

RESULTS

Regulation of PKC-α by 12(*S*)-HETE and 13(*S*)-HODE. Western blot using antibodies against PKC-α, -βI, -βII, -γ, -δ, -ε, or -ξ revealed that PKC-α protein was the only isoform detected in B16a cells, whereas all seven PKC isoforms were detected in C57BL/6J mouse brain tissue (data not shown).

12(*S*)-HETE (0.1 μM) treatment induced a rapid and transient increase in membrane-associated PKC-α in B16a cells. A 3-fold increase in the membrane-associated PKC-α was observed 5 min after 12(*S*)-HETE treatment (Fig. 1*A*). Pretreatment of B16a cells with 13(*S*)-HODE prior to 12(*S*)-HETE inhibited the 12(*S*)-HETE-increased association of PKC-α, with a complete inhibition at 1 μM 13(*S*)-HODE (Fig. 1*B*). Immunofluorescent studies using these cells also demonstrated that 12(*S*)-HETE induced a translocation of PKC-α from the cytosol to the plasma membrane, and vinculin-containing focal adhesion plaques and these 12(*S*)-HETE effects were abolished by 13(*S*)-HODE (data not shown). Further, Western blotting detected an 80-kDa PKC-α band in cytoskeletons isolated from 12(*S*)-HETE-treated B16a cells (Fig. 1*C*), and PKC activity of cytoskeleton from 12(*S*)-HETE-treated cells was four times that of control cells (Fig. 1*D*).

Analysis of the Mechanism of Action for Regulation of PKC-α by 12(*S*)-HETE and 13(*S*)-HODE. We first performed an *in vitro* activation assay using purified PKC-α in a mixed micelle system (21). No direct activation of PKC-α by 12(*S*)-HETE was observed (Fig. 2*A*). Next, we determined the effect of 13(*S*)-HODE on PMA activation of PKC-α in B16a cells. Pretreatment of cells with 13(*S*)-HODE (0.1 or 1 μM for 10 min) prior to PMA (50 nM for 10 min) treatment did not inhibit the PMA-induced PKC-α translocation (Fig. 2*B*). In addition, 13(*S*)-HODE did not inhibit PKC *in vitro* (data not shown). Thus, we concluded that neither 12(*S*)-HETE nor 13(*S*)-HODE exert a direct effect on PKC-α.

Hence we then investigated the effect of 12(*S*)-HETE and 13(*S*)-HODE on the generation of second messengers DAG and IP_3 in B16a cells. As shown in Fig. 2*C*, 12(*S*)-HETE treatment (0.1 μM) induced a rapid and transient increase in the level of DAG. A maximal increase in DAG (100% over control) was observed after treatment with 0.1 μM 12(*S*)-HETE for 2.5 min. Pretreatment of cells with 13(*S*)-HODE (10 min) prior to 12(*S*)-HETE (0.1 μM for 2.5 min) treatment blocked the 12(*S*)-HETE-induced increase in DAG formation, with a complete inhibition by 1 μM 13(*S*)-HODE (Fig. 2*C*). 13(*S*)-HODE alone (0.1–1 μM for 10 min) did not affect the level of DAG in these cells. In addition to DAG, a concomitant increase in IP_3 was observed after 12(*S*)-HETE treatment (Fig. 2*D*). A maximal increase in IP_3 (150% over control) was obtained by treatment of cells for 2.5–5 min with 0.1 μM 12(*S*)-HETE (Fig. 2*D*). Again, the 12(*S*)-HETE (0.1 μM for 2.5 min)-increased IP_3 generation was completely inhibited by 1 μM 13(*S*)-HODE, and 13(*S*)-HODE alone did not affect the level of IP_3 in B16a cells (Fig. 2*D*).

The observation that 12(*S*)-HETE triggered the formation of DAG and IP_3 suggested the involvement of a phosphatidylinositol-specific PLC. To assess this possibility, we tested whether a PLC inhibitor, U73122 (Biomol, Plymouth Meeting, PA), would block the 12(*S*)-HETE-increased adhesion of B16a

cells to fibronectin. The 12(*S*)-HETE-increased adhesion of B16a cells to fibronectin was time and dose dependent and was sensitive to inhibition by 13(*S*)-HODE and the PKC inhibitor calphostin C. Pretreatment of B16a cells with U73122 (0.33–3.3 μM for 10 min) prior to 12(*S*)-HETE (0.1 μM for 10 min) treatment inhibited, in a dose-dependent manner, the 12(*S*)-HETE-increased B16a adhesion to fibronectin. A complete inhibition was observed with 3.3 μM U73122 (Fig. 3*A*). In contrast, U73433, which is an ineffective analog of U73122 (23), failed to block the 12(*S*)-HETE-increased B16a adhesion to fibronectin (Fig. 3*A*). Neither inhibitor alone (3.3 μM) altered the basal adhesion of B16a cells to fibronectin (Fig. 3*A*). The 12(*S*)-HETE-increased adhesion of B16a cells to fibronectin was inhibited in a dose-dependent manner by pertussis toxin (3–100 ng/ml for 60 min; Fig. 3*B*). However, no inhibition was observed with cholera toxin (30–1000 ng/ml for 60 min). In addition, pretreatment of cells with the tyrosine kinase inhibitor genistein (1–10 μM for 10 min) prior to 12(*S*)-HETE (0.1 μM for 10 min) treatment did not inhibit the 12(*S*)-HETE-increased B16a cell adhesion (data not shown).

The above results suggested a receptor-mediated mechanism of action for 12(*S*)-HETE; therefore, B16a cells were analyzed for their ability to bind to 12(*S*)-HETE. As shown in Fig. 3*C*, a time-dependent binding of 12(*S*)-HETE by B16a cells was observed. The specific binding at 4°C was saturated 120 min after addition of 12(*S*)-HETE. Analysis of the dose-dependent binding data revealed two populations of binding sites with K_{d1} = 0.96 nM and K_{d2} = 95 nM (Fig. 3*D*). The number of binding sites per cell was calculated as 33,500 and 206,000 for the high- and low-affinity binding sites, respectively. Moreover, the binding of 12(*S*)-HETE to B16a cells was effectively blocked by 13(*S*)-HODE, with an approximate IC_{50} of 4 nM (Fig. 3*E*). Neither the enantiomer [12(*R*)-HETE] nor the positional isomers [5(*S*)-, 8(*S*)-, 11(*S*)-, or 15(*S*)-HETE] could block 12(*S*)-HETE binding (data not shown).

DISCUSSION

PKC has been shown to play a role in various stages of tumor metastasis. In the present study, we demonstrate that 12(*S*)-HETE induced a translocation of a specific PKC isoform (i.e., PKC-α) to focal adhesion plaques, in addition to the plasma membrane. Further, this 12(*S*)-HETE activation of PKC-α was antagonized by 13(*S*)-HODE. Our results with physiological modulators [i.e., 12(*S*)-HETE and 13(*S*)-HODE] are supported by studies using such pharmacological agents as PMA (24).

The underlying mechanism regulating the interaction among 12(*S*)-HETE, 13(*S*)-HODE, and PKC-α is not understood. A number of studies reported that arachidonic acid as well as 12(*S*)-HETE activated PKC *in vitro* (9, 10, 25). However, our studies suggest an indirect mechanism(s) of action for 12(*S*)-HETE/13(*S*)-HODE. First, we did not observe any direct activation of PKC-α by 12(*S*)-HETE. Second, 13(*S*)-HODE did not inhibit the cytosol-to-membrane translocation of PKC induced by PMA but inhibited translocation induced by 12(*S*)-HETE. Third, 12(*S*)-HETE triggered the formation of DAG and IP_3, and 13(*S*)-HODE blocked this 12(*S*)-HETE effect. Fourth, we detected specific high-affinity binding sites for 12(*S*)-HETE in B16a cells, and 13(*S*)-HODE effectively blocked the 12(*S*)-HETE binding.

Eicosanoid receptors have been identified for prostaglandin E (12–14), prostaglandin $F_{2\alpha}$ (15), prostacyclin (16), thromboxane A_2 (17), and leukotriene D_4 (18). Diverse and sometimes multiple signaling mechanisms are found to be associated with these receptors. For example, lipoxin A_4 appears to be utilizing a pathway coupled to a pertussis toxin-sensitive

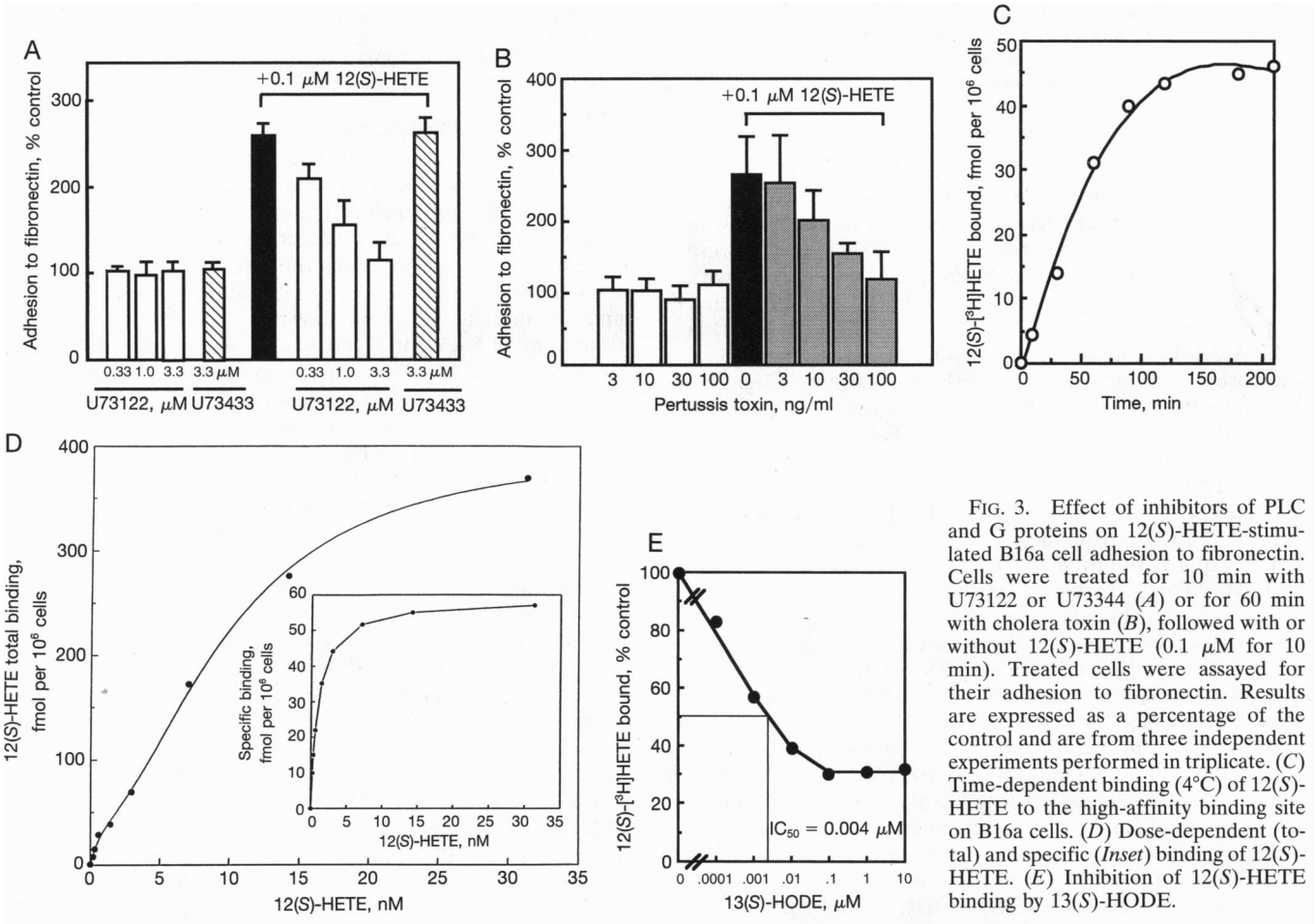

FIG. 3. Effect of inhibitors of PLC and G proteins on 12(*S*)-HETE-stimulated B16a cell adhesion to fibronectin. Cells were treated for 10 min with U73122 or U73344 (*A*) or for 60 min with cholera toxin (*B*), followed with or without 12(*S*)-HETE (0.1 μM for 10 min). Treated cells were assayed for their adhesion to fibronectin. Results are expressed as a percentage of the control and are from three independent experiments performed in triplicate. (*C*) Time-dependent binding (4°C) of 12(*S*)-HETE to the high-affinity binding site on B16a cells. (*D*) Dose-dependent (total) and specific (*Inset*) binding of 12(*S*)-HETE. (*E*) Inhibition of 12(*S*)-HETE binding by 13(*S*)-HODE.

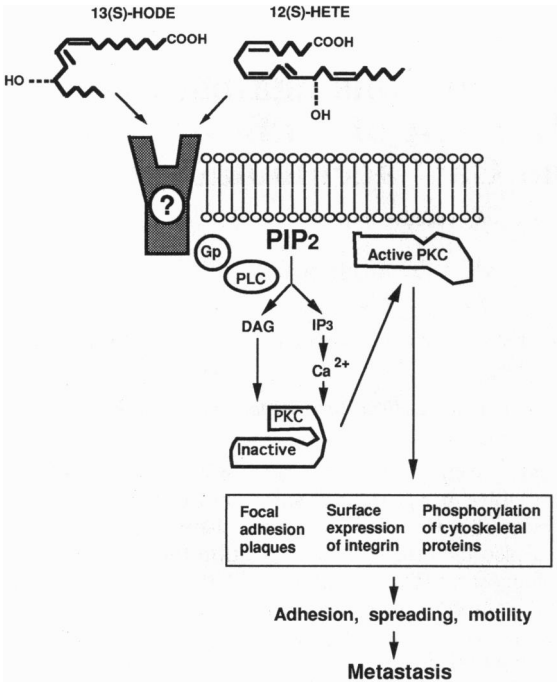

FIG. 4. Proposed mechanism of action for 12(*S*)-HETE and 13(*S*)-HODE regulation of PKC-α. Gp, G protein; PIP_2, phosphatidylinositol bisphosphate.

guanine nucleotide-binding protein (G protein) and leading to stimulation of phospholipase D (26). However, the G protein-linked leukotriene D4 appears to exert its effect by activating PLC-mediated inositol phospholipid breakdown (27), whereas binding of prostacyclin to its receptor leads to the formation of both cAMP and inositol phosphates (16).

Little is known about the receptors and related signaling pathways for HETEs and HODEs, although high-affinity binding sites for 12(*S*)-HETE have been described for several cell lines (28–30). In the present study using B16a cells, we report the existence of specific high-affinity binding sites for 12(*S*)-HETE. Further, we delineated the signaling pathway for 12(*S*)-HETE in that 12(*S*)-HETE triggers the formation of second messengers DAG and IP_3, which leads to the activation of PKC-α, and that this 12(*S*)-HETE-induced generation of DAG and IP_3 involves an inositol phospholipid-specific PLC and a pertussis toxin-sensitive G protein. We also demonstrated that 13(*S*)-HODE effectively competes with 12(*S*)-HETE for binding to the high-affinity binding site. In addition to this antagonistic effect, we cannot exclude the possibility that 13(*S*)-HODE may, through binding to its own yet undefined receptor, initiate a process that in turn inhibits the activation of PLC by 12(*S*)-HETE. Interestingly, Smith *et al.* (31) recently suggested that 15(*S*)-HETE might block receptor agonist-triggered cell signaling by direct inhibition of PLC or by uncoupling G protein stimulation of PLC. The analogy in mechanism of action between 15(*S*)-HETE and 13(*S*)-HODE awaits confirmation.

Our present studies support a receptor-mediated, G-protein- and PLC-linked mechanism of action for 12(*S*)-HETE. We cannot rule out the possibility of additional modes of action for 12(*S*)-HETE, depending on the site of generation. For example, 12(*S*)-HETE generated by one cell type may modulate, in a "cytokine" fashion, responses of adjacent cells, as suggested by studies with tumor cells, endothelial cells, and platelets (32, 33). In contrast, intracellularly generated 12(*S*)-HETE may directly activate PKC (10) or possibly other kinases. Finally, endogenously generated 12(*S*)-HETE may be released from cells to bind to a cell surface receptor as an "autocrine" mediator.

In conclusion, as summarized in Fig. 4, this study demonstrates that 12(*S*)-HETE interacts with its high-affinity binding sites, which leads to a G protein-linked and inositol phospholipid-specific PLC-mediated generation of DAG and IP_3. 13(*S*)-HODE competes with 12(*S*)-HETE for its binding to the receptor. Hence, 12(*S*)-HETE and 13(*S*)-HODE bidirectionally modulate the adhesion of B16a cells to extracellular matrix proteins through their regulation of the association of PKC-α to plasma membrane and focal adhesion plaques.

We thank R. Bazaz, C. Renaud, and S. Stojkovic for excellent technical assistance. This work was supported in part by National Institutes of Health Grants CA29997 (K.V.H.) and HL43702 (Y.A.H.).

1. Nishizuka, Y. (1992) *Science* **258,** 607–614.
2. Honn, K. V. & Tang, D. G. (1992) *Cancer Metastasis Rev.* **11,** 353–375.
3. Honn, K. V., Nelson, K. K., Renaud, C., Bazaz, R., Diglio, C. A. & Timar, J. (1992) *Prostaglandins* **44,** 413–429.
4. Grossi, I. M., Fitzgerald, L. A., Umbarger, L. A., Nelson, K. K., Diglio, C. A., Taylor, J. D. & Honn, K. V. (1989) *Cancer Res.* **49,** 1029–1037.
5. Timar, J., Chen, Q. Y., Liu, B., Bazaz, R., Taylor, J. D. & Honn, K. V. (1992) *Int. J. Cancer* **52,** 594–603.
6. Liu, B., Timar, J., Howlett, J., Diglio, C. A. & Honn, K. V. (1991) *Cell Regul.* **2,** 1045–1055.
7. Liu, B., Renaud, C., Nelson, K. K., Chen, Y. Q., Bazaz, R., Kowynia, J., Timar, J. & Honn, K. V. (1992) *Int. J. Cancer* **52,** 147–152.
8. Spector, A. A., Gordon, J. A. & Moore, S. A. (1988) *Prog. Lipid Res.* **27,** 271–323.
9. Hansson, A., Serhan, C. N., Haeggstrom, J., Ingelman-Sundberg, M., Samuelsson, B. & Morris, J. (1986) *Biochem. Biophys. Res. Commun.* **134,** 1215–1222.
10. Shearman, M. S., Naor, Z., Sekigucki, K., Kishimoto, A. & Nishizuka, Y. (1989) *FEBS Lett.* **243,** 177–182.
11. Herbertsson, H. & Hammarstrom, S. (1995) in *Eicosanoids and Other Bioactive Lipids in Cancer, Inflammation and Radiation Injury*, eds. Honn, K. S., Nigam, V., & Marnett, L. J. (Plenum, New York), in press.
12. Sugimoto, Y., Namba, T., Honda, A., Hayashi, Y., Negishi, M., Ichikawa, A. & Nurumiya, S. (1992) *J. Biol. Chem.* **267,** 6463–6466.
13. Honda, A., Sugimoto, Y., Namba, T., Watabe, A., Irie, A., Negishi, M., Narumiya, S. & Ichikawa, A. (1993) *J. Biol. Chem.* **268,** 7759–7762.
14. Funk, C. D., Furci, L., FitzGerald, G. A., Grygorczyk, R., Rochette, C., Bayne, M. A., Abramovitz, M., Adam, M. & Metters, K. M. (1993) *J. Biol. Chem.* **265,** 26767–26772.
15. Sakamoto, K., Ezashi, T., Miwa, K., Okuda-Ashitaka, E., Houtani, T., Sugimoto, T., Ito, S. & Hayaishi, O. (1994) *J. Biol. Chem.* **269,** 3881–3886.
16. Namba, T., Oida, H., Sugimoto, Y., Kakizuka, A., Negishi, M., Ichikawa, A. & Narumiya, S. (1994) *J. Biol. Chem.* **269,** 9986–9992.
17. Hirata, M., Hayashi, Y., Ushikubi, F., Yokota, Y., Kageyama, R., Nakanishi, S. & Narumiya, S. (1991) *Nature (London)* **349,** 617–620.
18. Watababe, T., Shimizu, T., Miki, I., Sakanaka, C., Honda, Z. I., Seyama, Y., Teramoto, T., Matsushima, T., Ui, M. & Kurokawa, K. (1990) *J. Biol. Chem.* **265,** 21237–21241.
19. Wetsel, W. C., Khan, W. A., Merchenthaler, I., Rivera, H., Halpern, A. E., Phung, H. M., Negro-Vilar, A. & Hannun, Y. A. (1992) *J. Cell Biol.* **17,** 121–133.
20. Blobe, G. C., Sachs, C. W., Khan, W. A., Fabbro, D., Stabel, S., Wetsel, W. C., Obeid, L. M., Fine, R. L. & Hannun, Y. A. (1993) *J. Biol. Chem.* **268,** 658–664.
21. Hannun, Y. A., Loomis, C. R. & Bell, R. M. (1985) *J. Biol. Chem.* **260,** 10039–10043.
22. Bligh, E. G. & Dyer, W. J. (1957) *Can J. Biochem. Physiol.* **37,** 911–917.
23. Thompson, A. K., Mostafapour, S. P., Denlinger, L. C., Bleasdale, J. E. & Fisher, S. K. (1991) *J. Biol. Chem.* **266,** 23856–23862.
24. Woods, A. & Couchman, J. R. (1992) *J. Cell Sci.* **102,** 277–290.
25. McPhail, L. C., Clayton, C. C. & Snyderman, R. (1984) *Science* **224,** 622–625.
26. Fiore, S., Ryeom, S. W., Weller, P. F. & Serhan, C. N. (1992) *J. Biol. Chem.* **267,** 16168–16176.
27. Sjolander, A., Gronroos, E., Hammarstrom, S. & Andersson, T. (1990) *J. Biol. Chem.* **265,** 20976–20981.
28. Suss, R., Arenberg, P., Gross, E. C. & Ruzicka, T. (1990) *Exp. Cell Res.* **191,** 204–208.
29. Herbertsson, H. & Hammarstrom, S. (1992) *FEBS Lett.* **298,** 249–252.
30. Gross, E., Ruzicka, T., Restorff, B. V., Stolz, W. & Klotz, K. N. (1990) *J. Invest. Dermatol.* **94,** 446–451.
31. Smith, R. J., Justen, J. M., Nidy, E. G., Sam, L. M. & Bleasdale, J. E. (1993) *Proc. Natl. Acad. Sci. USA* **90,** 7270–7274.
32. Honn, K. V., Tang, D. G., Grossi, I. M., Duniec, Z. M., Timar, J., Renaud, C., Leighauser, M., Blair, I., Johnson, C. R., Diglio, C. A., Kimler, V. A., Taylor, J. D. & Marnett, L. J. (1994) *Cancer Res.* **54,** 565–574.
33. Honn, K. V., Tang, D. G., Grossi, I. M., Renaud, C., Duniec, Z. M., Johnson, C. R. & Diglio, C. A. (1994) *Exp. Cell Res.* **210,** 1–9.